Original paper

Bouškaite, a new molybdenyl–hydrogensulfate mineral, $(MoO_2)_2O(SO_3OH)_2(H_2O)_2{\cdot}2H_2O$, from the Lill mine, Příbram ore area, Czech Republic

Jiří SEJKORA[1*], Ian E. GREY[2], Anthony R. KAMPF[3], Jakub PLÁŠIL[4], Pavel ŠKÁCHA[1,5]

[1] *Department of Mineralogy and Petrology, National Museum, Cirkusová 1740, 193 00 Prague 9, Czech Republic; jiri_sejkora@nm.cz*
[2] *CSIRO Mineral Resources, Private Bag 10, Clayton South, Victoria 3169, Australia*
[3] *Mineral Sciences Department, Natural History Museum of Los Angeles County, 900 Exposition Boulevard, Los Angeles, CA90007, USA*
[4] *Institute of Physics ASCR, v.v.i., Na Slovance 1999/2, 182 21 Prague 8, Czech Republic*
[5] *Mining Museum Příbram, Hynka Kličky Place 293, 261 01 Příbram VI, Czech Republic*
[*] *Corresponding author*

Bouškaite, $(MoO_2)_2O(SO_3OH)_2(H_2O)_2{\cdot}2H_2O$ is a new supergene post-mining mineral from the mine dump of the Lill shaft, the Březové hory ore district (Příbram), Czech Republic, associated with rhomboclase and unspecified X-ray amorphous Mo-rich blue phase. It was found in weathered quartz gangue with disseminated tiny grains of pyrite and a black X-ray amorphous Mo sulphide (likely jordisite). It forms colorless to light beige aggregates of randomly or radially arranged fibers up to 7 mm in length on the surface of quartz gangue fragments. Individual crystals are very narrow blades flattened on {001} and elongated along [100]. Bouškaite has a white to light grey streak, vitreous luster, and does not fluoresce under either short- or long-wave ultraviolet light. Cleavage is perfect on {001}, the Mohs hardness is ~2, and the fracture is uneven. Aggregates of the mineral are very brittle; thin blades (fibers) are somewhat flexible. The measured density is 2.40(2) g/cm^3; the calculated density is 2.38 g/cm^3. Bouškaite is optically biaxial positive, the indices of refraction are $\alpha = 1.504(2)$, $\beta = 1.605(2)$, $\gamma = 1.705(3)$ and $2V_{meas.} = 82(1)°$. The mineral is triclinic, space group $P\bar{1}$, $a = 5.581(3)$, $b = 9.572(1)$, $c = 14.425(4)$ Å, $\alpha = 97.43(1)°$, $\beta = 100.05(2)°$, $\gamma = 89.96(1)°$, $V = 752.2(5)$ Å^3, $Z = 2$. The seven strongest lines in the X-ray powder diffraction pattern are [*d* (Å)/*I(hkl)*]: 14.154/35(001), 7.078/100(002), 5.440/9(10$\bar{1}$), 4.838/7(101), 4.720/56(003), 4.010/7(102) and 3.240/10(10$\bar{4}$). The chemical analyses by electron microprobe yielded CaO 0.08, SiO_2 0.36, MoO_3 53.59, SO_3 29.43, $H_2O_{calc.}$ 16.71, total 100.17 wt. %. The empirical formula on the basis of 17 anions per formula unit is $(MoO_2)_{2.00}Ca_{0.01}O(SO_3OH)_{1.98}(SiO_4)_{0.03}(H_2O)_2{\cdot}2H_2O$. The unique crystal structure of bouškaite was solved from synchrotron single-crystal diffraction data and refined to $R_{obs} = 0.092$ for 499 reflections with $I > 3\sigma(I)$. The structure of bouškaite is built from $(MoO_2)_2O(SO_3OH)_2(H_2O)_2$ chains, oriented parallel to [010] and linked to one another by hydrogen bonding to H_2O molecules, Ow3 and Ow4 lying between the adjacent chains. The chains contain triangular clusters consisting of two Mo-centered octahedra and a S1-centred tetrahedron. The triangular clusters are connected by corner-sharing with a S2-centred tetrahedron. The Raman spectrum of bouškaite with tentative band assignments is reported. The mineral is named in honor of the prominent Czech mineralogist and geochemist Prof. Dr. Vladimír Bouška (1933–2000) of Charles University, Prague.

Keywords: bouškaite, new mineral, molybdenyl–hydrogensulfate, crystal structure, Raman spectroscopy, Příbram
Received: 2 May 2019; accepted: 28 August 2019; handling editor: F. Laufek
The online version of this article (doi: 10.3190/jgeosci.287) contains supplementary electronic material.

1. Introduction

The Příbram ore area is one of the most important regions of hydrothermal ore mineralization in the Czech Republic. The ore deposits are situated near the boundary of the Teplá–Barrandian Unit (in this area Upper Proterozoic to Cambrian) and the Central Bohemian Plutonic Complex. There are two main ore districts that are distinguished by their geological positions and characteristics of their hydrothermal mineralizations: the silver-bearing base-metal ore district Březové Hory and the complex uranium–(base-metal) ore district Příbram (Litochleb et al. 2003). Within the Březové Hory district and adjacent to the main central Březové Hory deposit, are located the smaller deposits Bohutín (SW part) and Černojamské (NE part).

Beginning in 1965, the mine dump of the Lill shaft (main shaft of the Černojamské deposit) was removed in several stages and after 2001 an industrial plant was built on the site. The mine dump material of the Lill shaft collected during removal has become the source of many rare and unusual minerals (e.g. Ondruš et al. 1990; Plášil et al. 2005, 2009; Sejkora et al. 2010). One of these minerals is a new species with an ideal formula of $(MoO_2)_2O(SO_3OH)_2(H_2O)_2{\cdot}2H_2O$. In this paper, we report its full description.

The new mineral is named bouškaite in honor of the prominent Czech mineralogist Prof. Dr. Vladimír Bouška (1933–2000) of the Faculty of Science, Charles University in Prague, for his contribution to mineralogy and geochemistry. Prof. Bouška is the author of more than 630 published papers focused on mineralogy (ore minerals, metamict minerals, recently formed minerals, organic minerals), gemology, geochemistry (especially that of coal) and natural glasses (tektites).

The new mineral and name have been approved by the Commission on New Minerals, Nomenclature and Classification of the International Mineralogical Association (IMA 2018-055). The holotype specimen is deposited in the collections of the Department of Mineralogy and Petrology of the National Museum in Prague, Cirkusová 1740, Prague 9, Czech Republic, catalog number P1P 24/2018. Crystals from the holotype used in this study are deposited in the collections of the Natural History Museum of Los Angeles County, 900 Exposition Boulevard, Los Angeles, CA 90007, USA, under catalogue number 66776.

2. Occurrence

Bouškaite was found on samples originating from the mine dump of the Lill shaft (total depth 454.4 m), which is located in the vicinity of Příbram, central Bohemia (GPS coordinates 49°41'49"N 14°0'1"E). The mine was in operation during 1857–1902 and 1961–1965 as the main shaft of the Černojamské deposit in the Březové Hory ore district. More than 60 mineral species are known to date from the Lill shaft and it is the type locality for znucalite (Ondruš et al. 1990). The full list of minerals recorded from this area is given on Mindat Database (Mindat 2019).

The new mineral was found in weathered quartz gangue with disseminated tiny grains of pyrite and a black X-ray amorphous Mo-sulphide (likely jordisite); rare rhomboclase and unspecified X-ray amorphous Mo-rich blue phase were also identified in the association. Bouškaite is a supergene mineral, probably relatively recently formed in the relatively dry parts of the mine dump material by weathering of primary jordisite and pyrite.

3. Physical and optical properties

Bouškaite occurs as randomly or radially arranged fibers up to 7 mm in length (Figs 1–2) formed by multiple subparallel intergrowths of very narrow blades (Figs 3–4) on weathered quartz gangue. Individual crystals are flattened on {001} and elongated along [100]. The dominant form is {001}; other likely forms based upon SEM images (Fig. 3) include prisms built from the pinacoids {010}, {011} and {01$\bar{1}$} and pinacoids {100} and {10$\bar{1}$}.

Bouškaite is colorless to light beige; crystal aggregates are opaque to translucent; individual acicular crystals are translucent to transparent. The mineral has a white to light grey streak and vitreous luster. It does not fluoresce under either short- or long-wave ultraviolet light. Cleavage on {001} is perfect, the Mohs hardness is ~2, and the mineral is brittle (aggregates) with an uneven fracture; thin blades (fibers) are somewhat flexible. The density 2.40(2) g/cm^3 was measured by flotation in methylene iodide – toluene. The calculated density is 2.38 g/cm^3 based on the empirical formula and unit-cell volume from single-crystal data. Bouškaite is optically biaxial positive, with α = 1.504(2), β = 1.605(2) and γ = 1.705(3) (measured in white light); $2V_{meas.}$ = 82(1)° based on direct measurements on a spindle stage, $2V_{calc.}$ = 82.05°. Dispersion is moderate, $r > v$; no pleochroism was observed. The optical orientation is X ^ **c** = 24°, Y ^ **a** = 20°, Z ^ **b** = 16°.

Fig. 1 Bouškaite fibers consisting of bundles of narrow blades on weathered quartz gangue, Lill shaft, Příbram; width of image 5.1 mm.

4. Chemical composition

Samples of bouškaite were analyzed with a Cameca SX-100 electron microprobe (National Museum, Prague) operating in the wavelength-dispersion mode

Fig. 2 Radially arranged bouškaite fibers on weathered quartz gangue, Lill shaft, Příbram; width of image 11 mm.

with an accelerating voltage of 15 kV, a specimen current of 5 nA, and a beam diameter of 5 μm. The following lines and standards were used: K_α: fluorapatite (Ca), wollastonite (Ca), celestine (S); L_α: wulfenite (Mo). Peak counting times (CT) were 20 s for main elements and 60 s for minor elements; CT for each background was one-half of the peak time. The raw intensities were converted to concentrations automatically using PAP (Pouchou and Pichoir 1985) matrix-correction software. The elements Al, As, Bi, Cl, Co, F, Fe, K, Na, Ni, P, Pb, Sb and V were sought, but found to be below their respective detection limits (*c.* 0.01–0.05 wt. %). Water content could not be analyzed directly because of the minute amount of material available; its presence was confirmed by Raman spectroscopy and calculated by stoichiometry (obtained from our crystal-structure study) on the basis of 17 anions *pfu*.

Table 1 gives the chemical composition of bouškaite from Příbram (mean of eleven determinations). Results of the chemical analyses correspond very well with the ideal formula $(MoO_2)_2O(SO_3OH)_2(H_2O)_2 \cdot 2H_2O$. The minor contents of Ca and Si do not exceed 0.02 and 0.07 *apfu,* respectively. The empirical formula of bouškaite based on 17 *apfu* is $(MoO_2)_{2.00}Ca_{0.01}O(SO_3OH)_{1.98}(SiO_4)_{0.03}(H_2O)_2 \cdot 2H_2O$. The ideal formula is $(MoO_2)_2O(SO_3OH)_2(H_2O)_2 \cdot 2H_2O$, which requires MoO_3 53.50, SO_3 29.76, H_2O 16.74, total 100.00 wt. %.

5. Raman spectroscopy

The Raman spectrum was collected in the range 4000–20 cm^{-1} using a DXR dispersive Raman Spectrometer

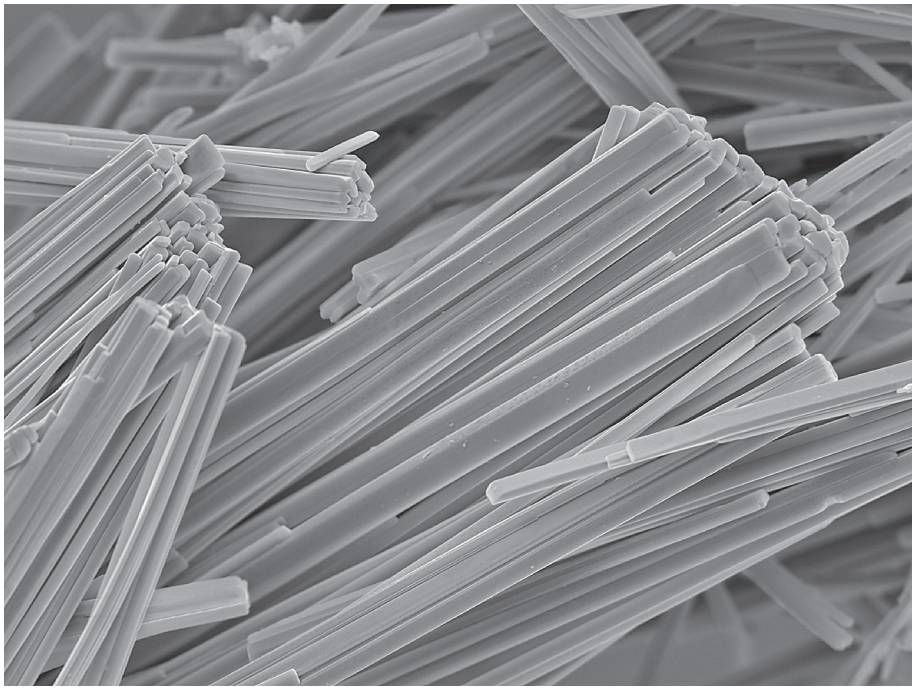

Fig. 3 Multiple subparallel intergrowths of narrow bouškaite blades; Lill shaft, Příbram; width of image 130 μm; SEM micrograph (BSE mode).

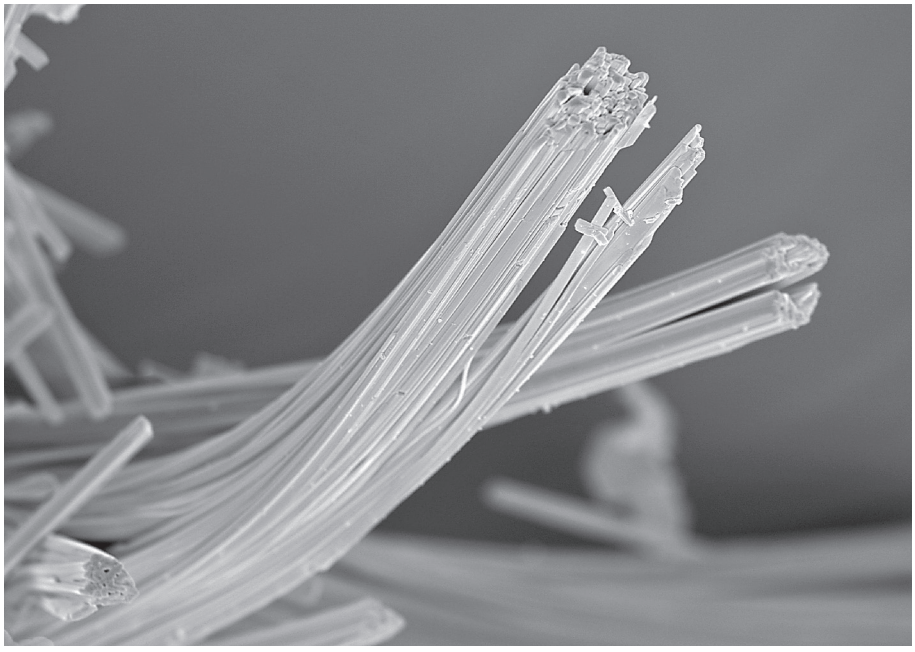

Fig. 4 Flexible bundles of narrow bouškaite blades; Lill shaft, Příbram; width of image 110 μm; SEM micrograph (BSE mode).

Tab. 1 Chemical composition of bouškaite from Příbram (wt. %)

constituent	mean 11 analyses	range	SD⁺
CaO	0.08	0–0.21	0.06
SiO_2	0.36	0–0.68	0.27
MoO_3	53.59	51.27–55.56	1.40
SO_3	29.43	26.39–32.06	1.63
H_2O*	16.71		
total	100.17		

⁺ Standard deviation

Note: content of H_2O* was calculated on the basis of the ideal composition [H_2O and (SO_3OH) groups] derived from the results of our crystal-structure study.

(Thermo Scientific) mounted on a confocal Olympus microscope. The Raman signal was excited by a green 532 nm diode-pumped solid-state laser and detected by a CCD detector. The experimental parameters were: 50× objective, 30 s exposure time, 100 exposures, 400 lines/mm grating, 25 μm pinhole spectrograph aperture and 2 mW laser power level. The spectra were repeatedly acquired from different grains in order to obtain a representative spectrum with the best signal-to-noise ratio. Possible thermal damage of the analysed region was excluded by visual inspection of the excited surface after measurement, by observation of possible decay of spectral features at the start of the excitation and by checking for thermal downshift of Raman lines. The instrument was set up using a software-controlled calibration procedure employing multiple neon emission lines (wavelength calibration), multiple polystyrene Raman bands (laser frequency calibration) and standardized white-light sources (intensity calibration). Spectral manipulations were performed using the Omnic 9 software (Thermo Scientific).

The Raman spectrum of bouškaite is shown in Fig. 5. The main bands observed are

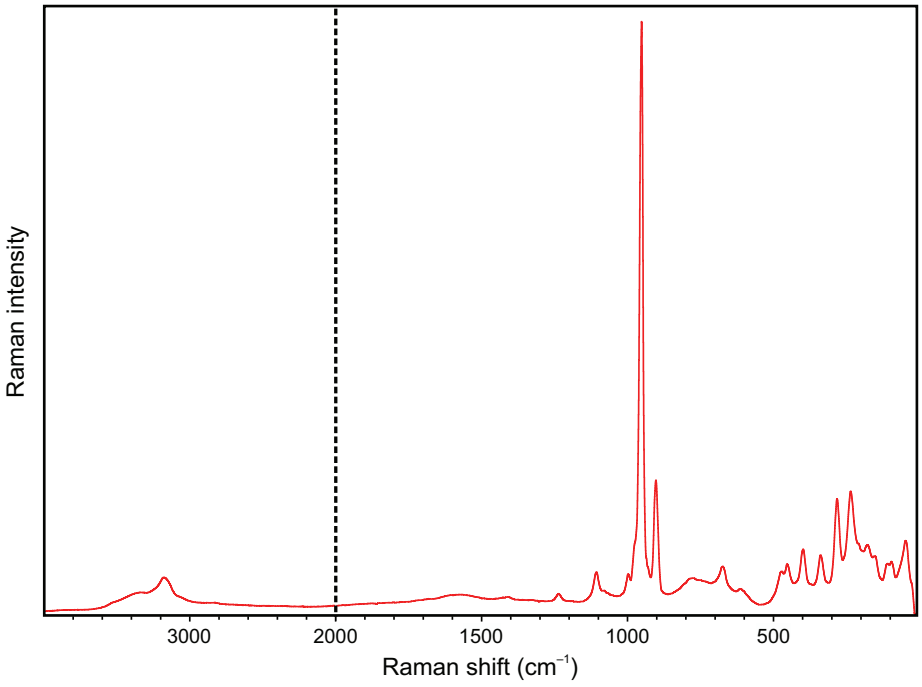

Fig. 5 Raman spectrum of bouškaite (split at 2000 cm^{-1}).

(in wavenumbers): 3529, 3355, 3170, 3046, 1583, 1412, 1235, 1107, 998, 974, 953, 949, 902, 778, 730, 672, 613, 475, 450, 399, 337, 282, 235, 206, 176, 149, 112, 93 and 49 cm^{-1}. The dominant bands in the 1000–800 cm^{-1} region (953, 949 and 902 cm^{-1}) can be assigned to stretching vibrations of short Mo=O bonds (Hardcastle and Wachs 1990; Daturi et al. 2001; Čejka et al. 2010), weaker bands at 337, 282 and 282 cm^{-1} and probably also [possible coincidence with bending vibrations of (SO_3OH) groups] at 613, 475 and 450 cm^{-1} may be related to vibration of Mo–O bonds. The vibrations of bonds of the (SO_3OH) group are observed at 1235, 1107 (ν_3 antisymmetric stretching), 998, 974 (ν_1 symmetric stretching), 672, 613 (ν_4 antisymmetric bending) and 475, 450, 399 cm^{-1} (ν_2 symmetric bending vibrations) (Gillespie and Robinson 1962; Haile et al. 1998; Plášil et al. 2013). The bands below 200 cm^{-1} are due to lattice modes. The presence of molecular water is documented by a broad OH-stretching band running from 3700 to 2700 cm^{-1} with components at 3596, 3355, 3170 and 3046 cm^{-1}; the presence of at least four distinct components in this area indicates several structurally non-equivalent water molecules. A weak and broad band at ~1583 cm^{-1} is assigned to the ν_2 (δ) bending vibrations of molecular H_2O.

Tab. 2 X-ray powder diffraction data (*d* in Å) for bouškaite from Příbram

$I_{obs.}$	$d_{obs.}$	$d_{calc.}$	*h*	*k*	*l*	$I_{obs.}$	$d_{obs.}$	$d_{calc.}$	*h*	*k*	*l*
34.5	14.154	14.158	0	0	1	0.6	2.4857	2.4873	2	1	1
0.8	9.477	9.475	0	1	0			2.4849	0	3	3
3.5	8.381	8.375	0	1	–1	0.2	2.4180	2.4191	2	0	2
1.5	7.453	7.455	0	1	1	0.7	2.3851	2.3855	0	4	–1
100.0	7.078	7.079	0	0	2	5.1	2.3589	2.3597	0	0	6
5.5	5.483	5.483	1	0	0	1.2	2.3180	2.3185	1	0	–6
8.6	5.440	5.441	1	0	–1	0.4	2.2539	2.2534	0	3	–5
7.4	4.838	4.838	1	0	1	0.6	2.2441	2.2441	2	2	1
55.6	4.720	4.719	0	0	3	0.4	2.2210	2.2224	0	3	4
7.0	4.010	4.011	1	0	2	2.0	2.2095	2.2099	2	0	3
1.6	3.929	3.930	1	0	–3	0.4	2.0918	2.0928	2	–3	0
0.4	3.815	3.814	1	–1	2			2.0911	2	3	–1
0.3	3.751	3.750	1	1	–3	0.3	2.0223	2.0226	0	0	7
1.1	3.721	3.727	0	2	2	0.4	2.0139	2.0145	1	0	–7
0.6	3.584	3.584	1	1	2	0.3	1.9799	1.9798	1	3	–6
4.3	3.578	3.575	0	2	–3	0.3	1.9573	1.9559	1	–3	–5
3.2	3.521	3.526	1	–2	–1	0.6	1.8935	1.8951	0	5	0
		3.521	1	–1	–3	1.2	1.8916	1.8908	0	5	–2
2.0	3.471	3.471	1	2	–2	1.2	1.8031	1.8028	1	–5	1
0.9	3.304	3.305	1	0	3	1.5	1.7984	1.7990	1	0	7
9.8	3.240	3.241	1	0	–4	0.2	1.7821	1.7820	2	0	–7
0.8	3.161	3.158	0	3	0	1.1	1.7694	1.7698	0	0	8
5.4	3.027	3.029	0	3	–2	1.3	1.7193	1.7177	3	–2	0
5.4	3.005	3.004	0	3	1	0.4	1.6995	1.6997	3	0	2
4.9	2.831	2.832	0	0	5	0.4	1.6522	1.6523	2	0	6
0.8	2.813	2.811	0	1	–5	0.2	1.6338	1.6337	1	3	–8
1.2	2.762	2.763	1	0	4			1.6337	0	3	–8
0.3	2.740	2.742	2	0	0	0.3	1.6310	1.6308	1	3	6
0.3	2.716	2.714	1	3	–2			1.6303	2	3	4
1.4	2.712	2.712	1	3	0	0.5	1.6201	1.6205	2	0	–8
0.6	2.701	2.700	1	–3	–1			1.6203	2	3	–7
0.5	2.624	2.624	0	1	5	0.3	1.6147	1.6150	1	–3	–7
0.7	2.609	2.608	2	0	1			1.6139	0	3	7
0.9	2.573	2.573	1	3	1	1.6	1.5911	1.5916	0	6	–1
0.5	2.556	2.555	1	–3	–2	0.2	1.5741	1.5731	0	0	9
0.3	2.518	2.519	0	3	–4						

6. X-ray powder diffraction

Powder X-ray diffraction (PXRD) data for bouškaite were collected at room temperature on a Bruker D8 Advance diffractometer (National Museum, Prague) with a solid-state 1D LynxEye detector using CuK_α radiation and operating at 40 kV and 40 mA. In order to minimize the background, the powder samples were placed on the surface of a flat silicon wafer in acetone suspension. We also collected data on the same diffractometer without acetone and the results were practically the same. The powder pattern was collected using Bragg–Brentano geometry in the range 3–70° 2θ, in 0.01° steps with a counting time of 20 s per step. Positions and intensities of reflections were found and refined using the PearsonVII profile-shape function with the ZDS program package (Ondruš 1993) and the unit-cell parameters were refined by the least-squares algorithm implemented by Burnham (1962). The experimental powder pattern was indexed in line with the calculated values of intensities obtained from the crystal-structure refinement, based on the Lazy Pulverix program (Yvon et al. 1977). The experimental powder data given in Tab. 2 agree well with the pattern calculated from the single-crystal data; experimental intensities are somewhat affected by a preferred orientation [001]. The refined unit-cell parameters of bouškaite are:

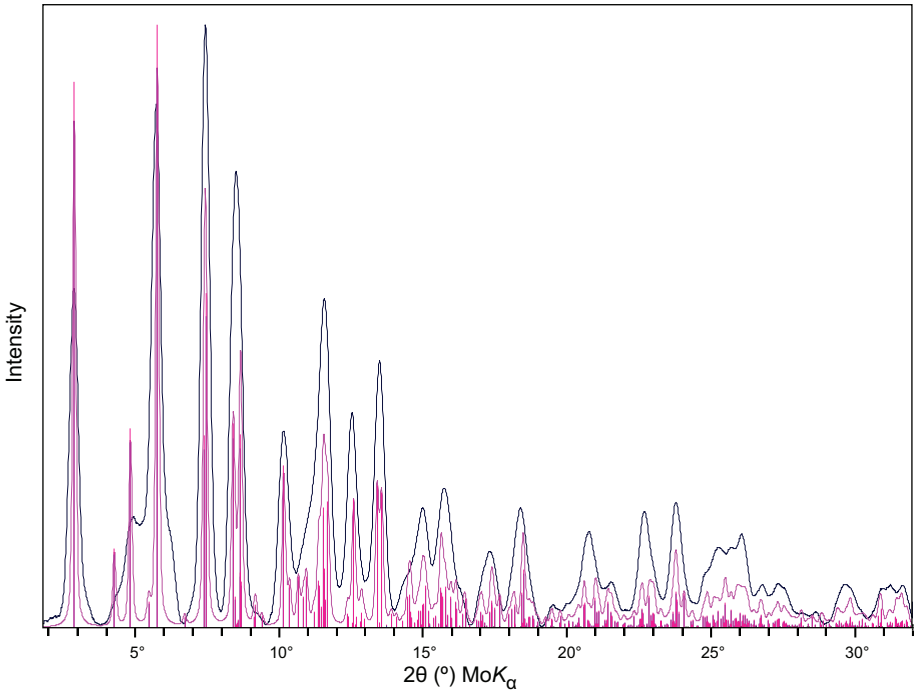

Fig. 6 Comparison of room-temperature powder XRD pattern for bouškaite (black line) with calculated pattern (red) based on the 100 K single-crystal structure.

$a = 5.5676(8)$, $b = 9.551(1)$, $c = 14.487(1)$ Å, $\alpha = 97.09(1)^o$, $\beta = 99.92(1)^o$, $\gamma = 89.99(1)^o$ and $V = 752.8(1)$ Å^3.

7. Single-crystal diffraction

A needle-shaped crystal of bouškaite (0.005 × 0.005 × 0.05 mm) was used for data collection on the macromolecular microfocus beamline MX2 of the Australian Synchrotron. Data were collected at 100 K with monochromatic wavelength, 0.7107 Å. A relatively high merging *R*-factor (12.2%) was obtained, which reflects the problem that even the finest needle crystals that could be selected under a binocular microscope are composed of subparallel fibres. In the crystal structure refinement using JANA2006 (Petříček et al. 2014), it was necessary to use the SKIP function to remove those reflections that were most affected by accidental overlap from different fibres. The MX2 beamline is used predominantly for proteins and other organic compounds and is operated at 100 K. We checked that the cooling did not cause changes to the crystal structure of bouškaite by collecting a PXRD pattern on unground crystals at 294 K and 45% relative humidity using a Rigaku R-Axis Rapid II curved imaging plate microdiffractometer with monochromatized MoK_α radiation and comparing with the pattern calculated from the crystal structure obtained at 100 K. A Gandolfi-like motion on the "φ and ω" axes was used to randomize the sample. The good agreement between the calculated and measured patterns is shown in Fig. 6.

Tab. 3 Crystal data and structure refinement for bouškaite

Formula	$(MoO_2)_2O(SO_3OH)_2(H_2O)_2 \cdot 2H_2O$	
Formula weight	538.1	
Temperature	100 K	
Wavelength	0.7107 Å	
Space group	$P\bar{1}$	
Unit-cell dimensions	$a = 5.581(3)$ Å	$\alpha = 97.430(10)°$
	$b = 9.5720(10)$ Å	$\beta = 100.05(2)°$
	$c = 14.425(4)$ Å	$\gamma = 89.960(10)°$
Volume	752.2(5) Å^3	
Z	2	
Absorption coefficient	2.03 mm^{-1}	
Crystal size	0.005 × 0.005 × 0.05 mm^3	
Theta range for data collection	1.45 to 32.1°	
Index ranges	$-7 \le h \le 7$, $-13 \le k \le 13$, $-19 \le l \le 19$	
Reflections collected	8412	
Resolution in refinement	0.92 Å	
Independent reflections	951 [$R_{int} = 0.122$]	
Reflections with $I_o > 3\sigma(I)$	492	
Refinement method	Full-matrix least-squares on F	
Data / restraints / parameters	951 / 0 / 85	
Final R indices [$I > 3\sigma(I)$]	$R_{obs} = 0.093$, w$R_{obs} = 0.096$	
R indices (all data)	$R_{obs} = 0.173$, w$R_{obs} = 0.110$	
Largest diff. peak and hole	0.94 and –1.04 e.Å^{-3}	

A structure solution in space group $P\bar{1}$ was obtained using SHELXT (Sheldrick 2015). Details of the data collection and refinement are given in Tab. 3. The refined coordinates, isotropic displacement parameters and bond-valence sums (BVSs) (Gagné and Hawthorne 2015) from the single crystal refinement are reported in Tab. 4. Selected interatomic distances are reported in Tab. 5. The H atoms could not be unambiguously located in difference-Fourier maps, but it is clear from the BVS values in Tab. 4 and the bond distances in Tab. 5 that Ow1 and Ow2 are coordinated water molecules, Ow3 and Ow4 are "free" water molecules, and the non-bridging sulphate-group ligands O2, O5 and O6 have significant hydroxyl character.

A [100] projection of the bouškaite structure is given in Fig. 7a. The structure is built from heteropolyhedral $(MoO_2)_2O(SO_3OH)_2(H_2O)_2$ chains oriented parallel to [010] and linked to one another by hydrogen bonding to H_2O molecules, Ow3 and Ow4 lying between the chains. The latter contain triangular clusters consisting of two Mo-centered octahedra and a S1-centred tetrahedron; the triangular clusters are connected by corner-sharing with a S2-centred tetrahedron. The two independent Mo-centered octahedra each have two short Mo=O and four long Mo-O distances (Tab. 5). This coordination geometry is typical of Mo^{6+} cations in natural and synthetic uranyl molybdates (Krivovichev and Burns 2000) and also occurs in structure of MoO_3 (Kihlborg 1963).

Tab. 4 Atom coordinates, isotropic displacement parameters (Å^2) and bond-valence sums (BVSs) for bouškaite

	x	*y*	*z*	U_{iso}	BVSs
Mo1	0.3042(3)	0.52983(19)	0.32050(13)	0.0173(7)	5.74
Mo2	0.3040(3)	0.89967(18)	0.31801(13)	0.0173(7)	6.00
S1	0.4442(9)	0.6763(6)	0.1300(4)	0.0196(12)	6.17
S2	0.5188(8)	1.2130(5)	0.3033(4)	0.0156(12)	5.87
O1	0.352(3)	0.6549(17)	0.0308(12)	0.032(4)	1.70
O2	0.711(2)	0.6857(15)	0.1539(10)	0.019(3)	1.51
O3	0.342(2)	0.8071(14)	0.1665(10)	0.019(3)	1.91
O4	0.359(3)	0.5572(15)	0.1761(10)	0.025(3)	1.79
O5	0.536(2)	1.2369(14)	0.4064(9)	0.018(3)	1.54
O6	0.752(3)	1.2079(17)	0.2712(12)	0.034(4)	1.57
O7	0.367(2)	1.0822(13)	0.2623(9)	0.013(3)	1.99
O8	0.365(3)	1.3188(16)	0.2525(11)	0.030(4)	1.83
O9	0.191(3)	0.4760(17)	0.4139(11)	0.032(4)	1.69
O10	0.601(3)	0.5639(18)	0.3621(12)	0.035(4)	1.91
O11	0.200(3)	0.9845(18)	0.4107(12)	0.035(4)	1.98
O12	0.612(2)	0.8753(15)	0.3617(10)	0.023(3)	1.55
O13	0.177(2)	0.7178(15)	0.3208(10)	0.022(3)	1.96
Ow1	–0.035(2)	0.9331(14)	0.2255(10)	0.020(3)	0.47
Ow2	–0.045(2)	0.4509(14)	0.2223(10)	0.019(3)	0.35
Ow3	0.048(3)	0.2520(19)	0.5083(13)	0.043(4)	0.00
Ow4	0.167(3)	0.318(2)	0.0433(14)	0.052(5)	0.00

A [010] projection of the structure in Fig. 7b shows the proposed hydrogen-bonding scheme in bouškaite. The coordinated water molecules, Ow1 and Ow2, are both hydrogen bonded to non-bridging sulphate-group ligands O2 and O6 in an adjacent heteropolyhedral chain. The "free" water molecules Ow3 and Ow4, each hydrogen bond to a non-bridging sulphate-group ligand in adjacent chains (O5 and O1, respectively), together with hydrogen bonds to O10/O12 and O4, respectively. The anion-pair separations involved in the hydrogen bonding are given in Tab. 5, together with the O–Ow–O angles, which have values that are conducive to hydrogen bonding.

8. Relationship to other species

Bouškaite is the member of Nickel–Strunz class 7.CB: Sulfates (selenates, etc.) without additional anions, with H_2O, with only medium-sized cations. It has a novel structure type and it does not correspond to any unnamed mineral species or synthetic compound.

Tab. 5 Polyhedral bond-lengths (Å), O–Ow–O angles (°) and likely hydrogen-bonded anions in bouškaite

Mo1–O4	2.205(16)	S1–O1	1.422(16)
Mo1–O8	2.182(15)	S1–O2	1.469(14)
Mo1–O9	1.720(18)	S1–O3	1.449(14)
Mo1–O10	1.677(15)	S1–O4	1.509(17)
Mo1–O13	1.933(14)	Av.	1.462
Mo1–Ow2	2.266(12)		
Av.	1.997	S2–O5	1.461(14)
		S2–O6	1.453(17)
Mo2–O3	2.296(14)	S2–O7	1.507(13)
Mo2–O7	2.071(14)	S2–O8	1.507(16)
Mo2–O11	1.665(17)	Av.	1.482
Mo2–O12	1.750(13)		
Mo2–O13	1.887(14)		
Mo2–Ow1	2.164(13)		
Av.	1.972		
Ow1…O2	2.75	Ow2…O2	2.82
Ow1…O6	2.93	Ow2…O6	2.81
O2-Ow1-O6	125.8	O2–Ow2–O6	128.1
Ow3…O5	2.97	Ow4…O1	2.93
Ow3…O10	2.88	Ow4…O4	2.86
Ow3…O12	2.82		
O5–Ow3–O10	142.6	O1–Ow4–O4	111.9
O5–Ow3–O12	144.1		

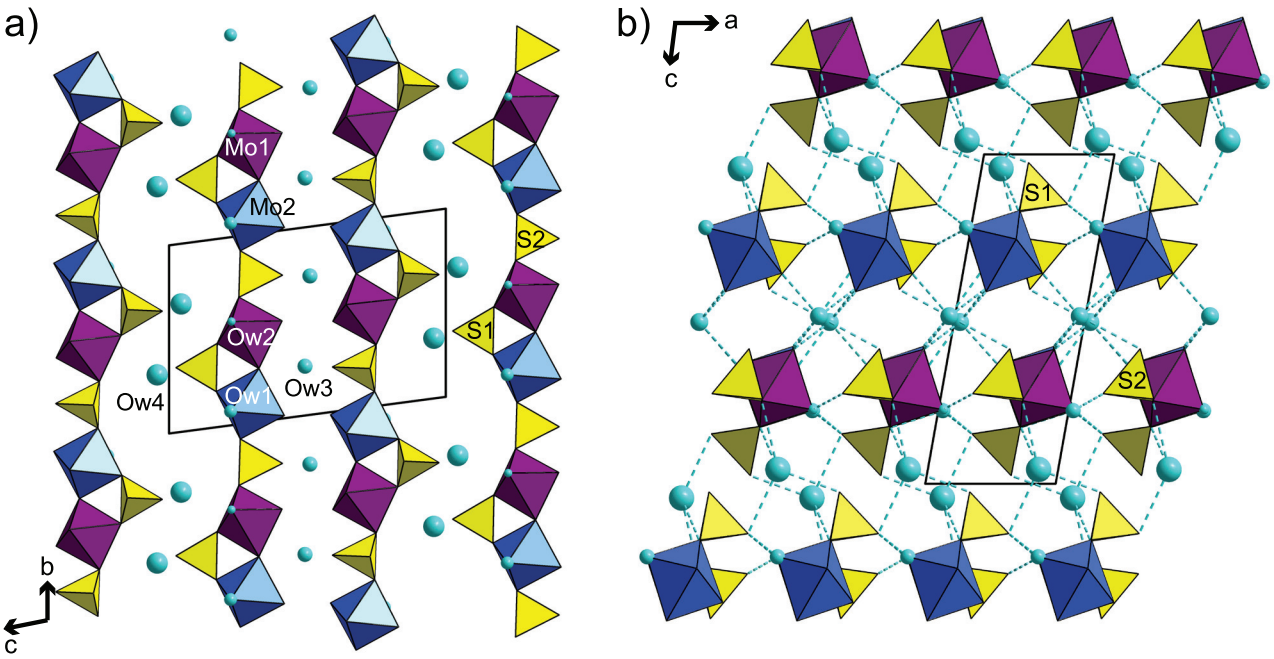

Fig. 7 Crystal structure of bouškaite projected along [100] (**a**) and [010] (**b**), displaying possible hydrogen-bonding scheme (blue dashed lines). Blue spheres represent O atoms of the molecular H_2O; thermal ellipsoids are displayed at the 75% probability level. Unit-cell edges are outlined in black solid lines. Yellow tetrahedra represent SO_4, violet octahedra $Mo(1)O_5(H_2O)$ and blue octahedra $Mo(2)O_5(H_2O)$.

A similar molybdenyl group has been reported in the crystal structure of vajdakite, $[(Mo^{6+}O_2)_2(H_2O)_2\ As^{3+}{}_2O_5]\cdot H_2O$ (Ondruš et al. 2002). The Gladstone–Dale compatibility index (Mandarino 1981) $1–(K_p/K_c)$ is –0.097 (poor) based upon the empirical formula, density calculated using the single-crystal cell and the measured indices of refraction. Similar poor Gladstone–Dale compatibilities found in heteropolymolybdates (Kampf et al. 2012) suggest that the Gladstone–Dale constant for Mo^{6+} (MoO_3) may need revising, particularly when short Mo=O bonds are involved.

Acknowledgements. This research was undertaken in part using the MX2 beamline at the Australian Synchrotron, part of ANSTO, and made use of the Australian Cancer Research Foundation (ACRF) detector. The authors acknowledge help from the beamline scientists for collection of the single-crystal X-ray data. The authors wish to express their thanks to Zdeněk Dolníček (National Museum, Prague) for his kind support of this study. The editor-in-chief Vojtěch Janoušek, handling editor František Laufek, an anonymous reviewer and Uwe Kolitsch, are acknowledged for valuable comments and suggestions that helped to improve the manuscript. This work was financially supported by Czech Science Foundation (project GACR 17-09161S).

Electronic supplementary material. Supplementary crystallographic data are available online at the Journal web site (*http://dx.doi.org/10.3190/jgeosci.287*).

References

Burnham CW (1962) Lattice constant refinement. Carnegie Inst Washington Yearbook 6: 132–135

Čejka J, Bahfenne S, Frost RL, Sejkora J (2010) Raman spectroscopic study of the arsenite mineral vajdakite $[(Mo^{6+}O_2)_2(H_2O)_2As^{3+}{}_2O_5]\cdot H_2O$. J Raman Spectrosc 41: 74–77

Daturi M, Busca G, Guesdon A, Borel MM (2001) Vibrational spectra study of Mo(V) phosphates as examples of different geometries of dimolybdenyl species. J Mater Chem 11: 1726–1731

Gagné OC, Hawthorne FC (2015) Comprehensive derivation of bond-valence parameters for ion pairs involving oxygen. Acta Crystallogr B71: 562–578

Gillespie RJ, Robinson EA (1962) The Raman spectra of sulphuric, deuterosulphuric, fluorosulphuric, chlorosulphuric, and methansulphonic acids and their anions. Can J Chem 40: 644–657

Haile SM, Calkins PM, Boysen D (1998) Structure and vibrational spectrum of β-$Cs_3(HSO_4)_2[H_{2-x}(P_{1-x}, S_x)O_4]$ (x~0.5), a new superprotonic conductor, and a comparison with α-$Cs_3(HSO_4)_2(H_2PO_4)$. J Solid State Chem 139: 373–387

Hardcastle FD, Wachs IE (1990) Determination of molybdenum-oxygen bond distances and bond orders by Raman spectroscopy. J Raman Spectrosc 21: 683–691

Kampf AR, Mills SJ, Rumsey MS, Dini M, Birch WD, Spratt J, Pluth JJ, Steele IM, Jenkins RA, Pinch

WW (2012) The heteropolymolybdate family: structural relations, nomenclature scheme and new species. Mineral Mag 76: 1175–1207

Kihlborg L (1963) Least-squares refinement of crystal structure of molybdenum trioxide. Arkiv Kemi 21: 357−364

Krivovichev SV, Burns PC (2000) Crystal chemistry of uranyl molybdates. I. The structure and formula of umohoite. Canad Mineral 38: 717–726

Litochleb J, Černý P, Litochlebová E, Sejkora J, Šreinová B (2003) The deposits and occurrences of mineral raw material in the Střední Brdy Mts. and the Brdy piedmont area (Central Bohemia). Bull mineral-petrolog Odd Nár Muz (Praha) 11: 57–86 (in Czech)

Mandarino JA (1981) The Gladstone-Dale relationship: Part IV. The compatibility concept and its application. Canad Mineral 19: 441–450

Mindat (2019) Příbram District. Accessed on April 24, 2019 at *https://www.mindat.org/loc-779.html*.

Ondruš P (1993) A computer program for analysis of X-ray powder diffraction patterns. Materials Science Forum, EPDIC-2, Enschede, 133–136, 297–300

Ondruš P, Veselovský F, Rybka R (1990) Znucalite, $Zn_{12}(UO_2)Ca(CO_3)_3(OH)_{22}\cdot 4H_2O$, a new mineral from Příbram, Czechoslovakia. Neu Jb Mineral, Mh 1990: 393–400

Ondruš P, Skála R, Císařová I, Veselovský F, Frýda J, Čejka J (2002) Description and crystal structure of vajdakite, $[(Mo^{6+}O_2)_2(H_2O)_2\ As^{3+}{}_2O_5]\cdot H_2O$ – a new mineral from Jáchymov, Czech Republic. Amer Miner 87: 983–990

Petříček V, Dušek M, Palatinus L (2014) Crystallographic computing system JANA2006: general features. Z Kristallogr 229: 345–352

Plášil J, Sejkora J, Litochleb J, Goliáš V (2005) A find of an andorite-like mineral (so-called "minéral F") in association with diaphorite and other Pb–Ag–Sb minerals on the mine dump of the Lill mine (Černojamské deposit), Příbram, Czech Republic. Bull mineral-petrolog Odd Nár Muz (Praha) 13: 187–192 (in Czech)

Plášil J, Sejkora J, Litochleb J, Škácha P (2009) The occurrence of rare Ag–Hg sulfide – imiterite – in dump material of the Lill mine (Černojamské deposit), the Březové Hory base-metal ore district, Příbram (Czech Republic). Bull mineral-petrolog Odd Nár Muz (Praha) 17: 62–68 (in Czech)

Plášil J, Kampf AR, Kasatkin AV, Marty J, Škoda R, Čejka J (2013) Meisserite, $Na_5(UO_2)(SO_4)_3(SO_3OH)(H_2O)$, a new uranyl sulfate mineral from the Blue Lizard mine, San Juan County, Utah, USA. Mineral Mag 77: 2975–2988

Pouchou JL, Pichoir F (1985) "PAP" (φρZ) procedure for improved quantitative microanalysis. In: Armstrong JT (ed) Microbeam Analysis. San Francisco Press, San Francisco, pp 104–106

Sejkora J, Černý P, Černý P (2010) The occurrence of rare selenate, munakaraite, at mine dump of the Lill mine, Příbram (Czech Republic). Bull mineral-petrolog Odd Nár Muz (Praha) 18: 87–90 (in Czech)

Sheldrick GM (2015) Crystal structure refinement with *SHELXL*. Acta Crystallogr C71: 3−8

Yvon K, Jeitschko W, Parthé E (1977) Lazy Pulverix, a computer program for calculation of X-ray and neutron diffraction powder patterns. J Appl Crystallogr 10: 73–74